TECHNICAL MEMORANDUM

524

Ku-Band Radar Altimeter Surface Wind Speed Algorithm

Saleh Abdalla

Research Department

April 2007

Series: ECMWF Technical Memoranda

A full list of ECMWF Publications can be found on our web site under:
http://www.ecmwf.int/publications/

Contact: library@ecmwf.int

Abstract

An algorithm for the retrieval of surface wind speed from Ku-band altimeter backscatter coefficient is proposed. The algorithm was derived using two-month (January-February 2005) worth of ENVISAT altimeter (RA-2) Ku-band backscatter data collocated with ECMWF model and buoy surface wind speeds. The algorithm was extensively verified using several collocated data sets including the altimeter Ku-band backscatter coefficient from ENVISAT, ERS-2 and Jason-1 and the wind speed from ECMWF model and from buoy observations over several years. The new algorithm increases altimeter wind speeds by about 0.40 m·s^{-1} and reduces the scatter index by about 5% compared to the well-known "modified Chelton-Wentz" algorithm. The algorithm performs even better than the two-parameter algorithm implemented for Jason-1 altimeter. The proposed algorithm was implemented for ENVISAT RA-2 on 24 October 2005. Verifications over a year afterwards showed better performance in terms of wind speed retrieval. The use of significant wave height as a second parameter for the altimeter wind retrieval algorithms may not be a proper choice for high sea-state conditions. It seems that the backscatter coefficient saturates for each significant wave height which can not be exceeded irrespective of the wind speed.

1. Introduction

A radar altimeter (RA) instrument is a nadir looking active device that is capable of measuring, with high precision, the time delay, the power and the shape of the radar pulses after reflection from the Earth surface. The time delay is proportional to the altitude of the instrument. The power and the shape of the reflected signal contain information on the characteristics of the surface that caused the reflection. Over the ocean, the shape of the reflected signal can be translated into significant wave height, H_s, while its power (the backscatter coefficient, σ^o) can be translated into ocean surface wind (defined here as the wind speed at a height of 10 m above the mean sea surface, U_{10}). Several satellites carrying RA instruments were launched during the last few decades. The list includes SEASAT, GEOSAT, TOPEX/Poseidon (usually referred to as TOPEX), ERS-1, ERS-2, Jason-1, GEOSAT Follow-On (GFO) and ENVISAT. All those platforms carry at least a Ku-band altimeter. Some satellites like ENVISAT and Jason-1 carry a second altimeter operating with a different radar frequency (S-band for ENVISAT and C-band for Jason-1). Hereafter, only Ku-band altimeter is considered.

Although there are several satellite-borne instruments capable of measuring higher density wind vector fields across rather wide swath (e.g. scatterometer), RA wind speed is still of great value for several applications like the correction of the altimeter estimate of mean sea surface height (e.g. the electromagnetic bias correction). RA wind speed data are very useful for monitoring the quality of model wind speeds. For example, at the European Centre for Medium-Range Weather Forecasts (ECMWF) the scatterometer wind speeds from both ERS-2 and QUIKSCAT, the buoy winds and the SSM/I (Special Sensor Microwave Imager) winds are assimilated in the atmospheric model. Therefore, these sources of data can not be used for independent verification of the model winds. Altimeter winds are also used for climatological studies (e.g. Young, 1999).

There are several empirical models for translating the Ku-band RA backscatter into ocean surface wind speed. The modified Chelton-Wentz (MCW) algorithm proposed by Witter and Chelton (1991) is the mostly used in operational retrieval from Ku-band altimeters. It is the one adopted for several altimeters like the ones onboard TOPEX, ERS-1, ERS-2 and ENVISAT (before late October 2005). The algorithm, which was devised based on a limited number of GEOSAT altimeter-buoy collocations, consists of a look-up table relating U_{10} to σ^o. Although this algorithm is generally performing rather satisfactorily, it was always felt that

there was room for improvement. Some improvement attempts refined the existing one-parameter algorithm (e.g. Freilich and Challenor, 1994) while others tried to introduce a sea-state dependence by including measured H_s as a second parameter (e.g. Gourrion et al., 2002) in retrieval algorithms. The sea-state dependence itself was the subject of several research efforts (e.g. Glazman and Greysukh, 1993 and Hwang et al., 1998). The results of those studies show ranges of impacts from significant to no impact (e.g. Wu, 1999). Some related discussion will be provided in Section 6 concerning this issue. For the purpose of the current work, the sea-state dependence will not be taken into account. It will be shown that the use of significant wave height as a proxy for sea-state dependence may not be a good choice when H_s is in excess of about 1.5-2.0 m.

The motivations for this effort are given in Section 2. The approach and the data set used to tune the algorithm are explained in Section 3. The results of the verification of the proposed algorithm are provided in Section 4. The proposed algorithm was implemented to ENVISAT RA-2 wind speed processing on 24 October 2005. Section 5 presents this implementation together with some results from the new implementation. Next, the issue of using the significant wave height as a proxy for sea-state dependence is discussed in Section 6. Finally, the conclusions are presented in Section 7.

2. Motivations:

More than two years of operational monitoring of the near real time ENVISAT Radar Altimeter-2 (RA-2) surface wind speed product suggested that the implemented wind speed retrieval algorithm, namely the MCW, needs to be fine-tuned. Fig. 1 shows a whole year of global comparison between RA-2 and ECMWF model wind speeds as a density scatter plot. One can clearly identify the need of tuning at low wind speeds (below ~5 m·s^{-1}) and at high wind speeds (above ~20 m·s^{-1}). The latter shortcoming is due to the limitation of the MCW look-up table that restricts the maximum wind speed value to around 20 m·s^{-1}. A similar picture emerges when comparing the wind speeds from RA-2 and the buoy measurements (which are received through the Global Telecommunication System, GTS) as can be seen in Fig. 2 for slightly more than a year. It is worthwhile mentioning that the buoys are mainly located in the Northern Hemisphere. Only buoys also reporting ocean wave data are used for the algorithm tuning and for the verification. The buoy wind speed observations were corrected based on the anemometer height. The procedure used by Bidlot et al. (2002) was adopted in this work. The RA-2 underestimation at low wind speed regime compared to buoys extends up to ~10 m·s^{-1}. It is worthwhile mentioning that the same picture emerges from the comparison between Jason-1 RA wind speed from one side and, on the other side, the ECMWF model (not shown) or the buoy winds as shown in Fig. 3, which covers a period of slightly less than two years. Keeping in mind that Jason-1 wind speed retrieval is based on the two-parameter algorithm, $\sigma^o = f(U_{10}, H_s)$, of Gourrion et al. (2002) one can question if H_s is enough to represent the sea-state dependence. Of course, the possibility that the algorithm of Gourrion et al. (2002) needs further tuning cannot be ruled out.
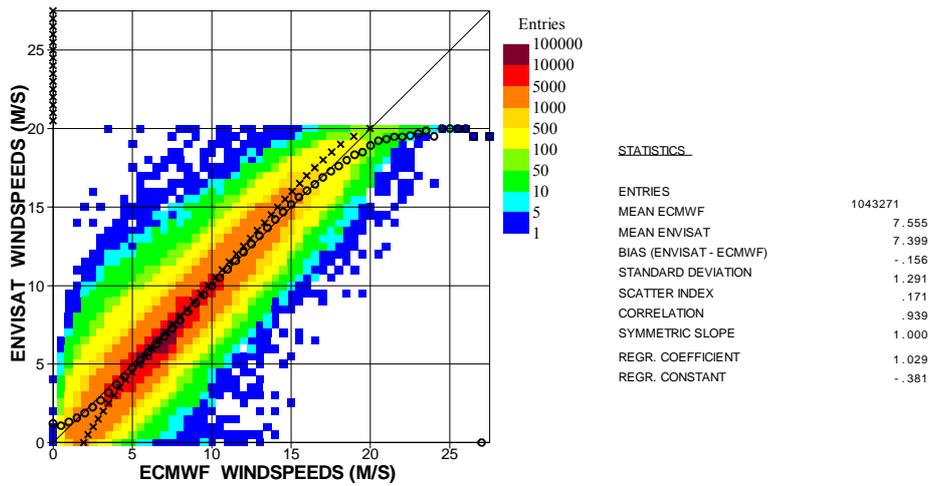
Figure 1: Global comparison between RA-2 and ECMWF model analysis wind speed values during the period from 1 September 2004 to 31 August 2005. The crosses (×) represent the average of "y" (RA-2 wind speed) for given "x" (i.e. ECMWF wind speed) and the circles (o) are vice versa.
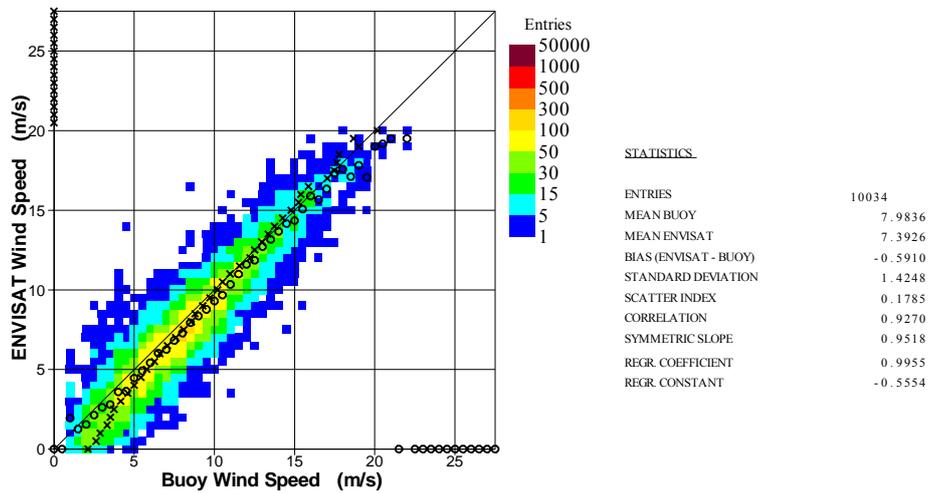
Figure 2: Global comparison between ENVISAT RA-2 and buoy wind speed values during the period from 1 January 2004 to 28 February 2005 (mainly in the NH). For the crosses and the circles see Fig. 1.
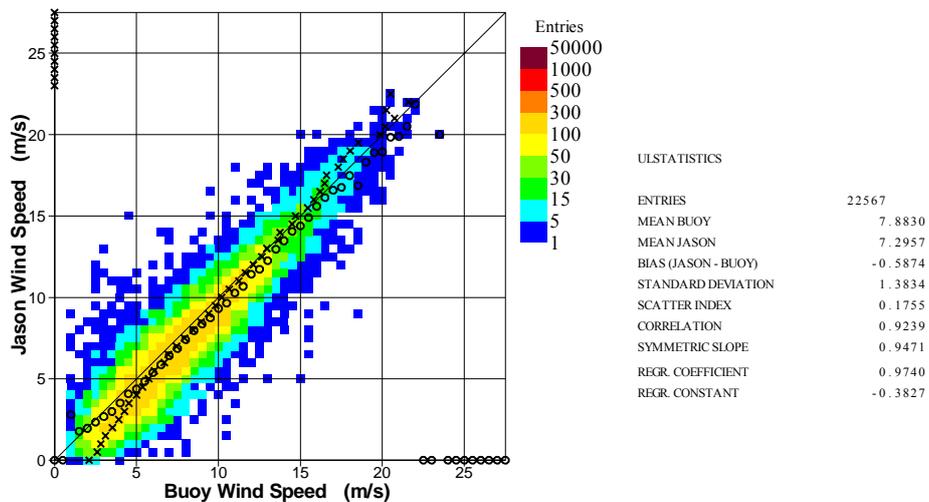
Figure 3: Global comparison between Jason RA and buoy wind speed values during the period from 1 October 2003 to 31 August 2005 (mainly in the NH). For the crosses and the circles see Fig. 1.

The need for improvement was also motivated by the comparison of the normalised histograms of occurrence of wind speeds from the altimeters and the collocated model counterparts (Fig. 4 and 5) or the collocated buoy (Fig. 5) winds. Fig. 5 represents the histograms for the collocations of RA-2 and buoy data sets together with the corresponding ECMWF model data. During a whole year only a limited number of collocations (less than 10000) were possible leading to the non-smooth shape of the histograms. It is interesting to notice that the model and the buoy histograms agree very well with each other (except for winds between 4 to 6 m·s^{-1}). This good agreement may be a consequence from the assimilation of the buoy winds into the ECMWF atmospheric model. Deviations of the RA-2 histograms from both model and buoy curves can not be missed in both Fig. 4 and Fig. 5.
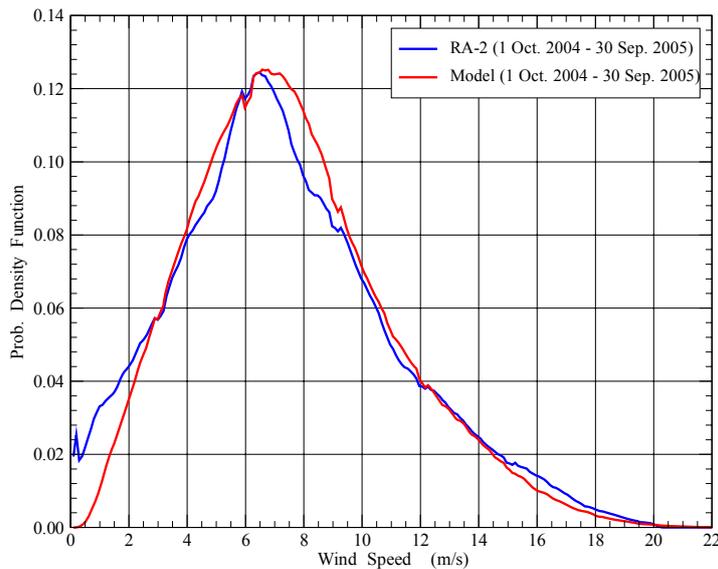
Figure 4: Probability density function of global wind speed from ENVISAT RA-2 (blue) and the corresponding ECMWF model collocations (red) during the period from 1 October 2004 to 30 September 2005.
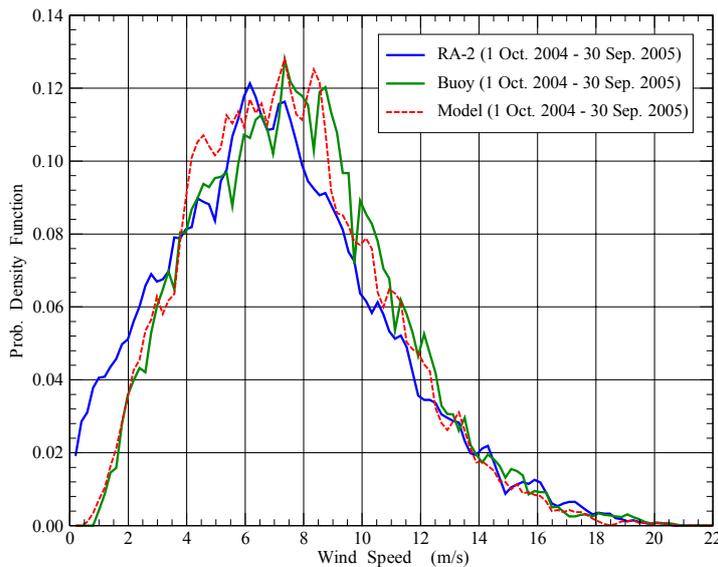
Figure 5: Probability density function of global wind speed from ENVISAT RA-2 (blue), from buoy (green) and the corresponding ECMWF model (red dashed) for the altimeter-buoy collocations during the period from 1 October 2004 to 30 September 2005.

3.   Algorithm tuning

Two months (January and February 2005) of global collocations between ENVISAT RA-2 backscatter coefficient, σ^o, and ECMWF model wind speed, U_{10}, were used for the algorithm tuning. While collocating various sources of data, it is important to ensure comparable scales (c.f. Janssen et al., 2003). The ECMWF model at the time had a horizontal resolution of about 40 km (TL511). Horizontal diffusion in the atmospheric model reduces considerably activity at the short scales. This increases the effective model scale which can be estimated to be in the order of 70 km. On the other hand, the distributed ENVISAT RA-2 Fast Delivery Marine Abridged Records Product (FDMAR) consists of 1-Hz observations, which are in fact the average of 20 individual echoes collected during 1 second. Therefore one expects the RA-2 scale to be around 7 km (the foot print corresponding to 1 Hz observations). However, due to the smoothing process of the tracking results over several consecutive observations the scale is larger. For the purpose of the current study, it is found that a satellite "super-observation" represented by an average of 11 consecutive (1-Hz) RA-2 observations can be of a comparable scale as that of the model. After proper quality control (similar to the one used by Abdalla and Hersbach, 2004, for ERS-2 RA), the total number of collocations used for the algorithm tuning is around 163,000.

While correlating the altimeter backscatter to the model wind speed, one needs to keep in mind that both the altimeter and the model suffer from various kinds of errors. It would be incorrect to assume that any of them is free of error. Instrumental errors (e.g. instrument calibration) and errors due to ambient conditions are examples for the possible sources of errors in the altimeter backscatter measurements. On the other hand, imperfect model physics, parameterisation and numerics are responsible for errors in model winds. Assuming the errors are normally distributed around the truth, one can make use of averaging in a hope that enough volume of data leads to means closer to the truth.

The scatter plot between σ^o and U_{10} is highly scattered (not shown). The backscatter coefficient range was divided into bins of 0.1 dB. All collocated model U_{10} values within each bin were averaged. The results are plotted as blue dots in Fig. 6 providing the number of collocations in the bin is more than 35. Similarly, the wind speed range was binned into 0.1 m·s^{-1} bins and the collocated σ^o values are averaged within each bin. The results are plotted as red crosses in Fig. 6 for bins with more than 35 collocations. A two segment function was fitted to the data in the form:

$$U_m = \begin{cases} \alpha - \beta\sigma^o & \text{if } \sigma^o \leq \sigma_b \\ \gamma \exp(-\delta\sigma^o) & \text{if } \sigma^o > \sigma_b \end{cases} \tag{1}$$

where U_m is a first-guess estimation of U_{10} while $\alpha, \beta, \gamma, \delta$ and σ_b are parameters to be found by fitting. While fitting a two-segment function, one needs to consider the continuity of the function and, at least, its first derivative at the breaking point σ_b. Linear regression was done for the linear segment. For the exponential segment, nonlinear curve fitting was used. A weighting function inversely proportional to (the sixth power of) σ^o values was used to favour the densely populated middle part of the function. Neutral regression was used by fitting $U_m = f_1(\sigma^o)$ and $\sigma^o = f_2(U_m)$ and then the golden mean is considered. The following values were obtained:

$$\alpha = 46.5 \quad \beta = 3.6 \quad \gamma = 1690 \quad \delta = 0.5 \quad \text{and} \quad \sigma_b = 10.917 \text{ dB} \tag{2}$$

Irrespective of the current accuracy of the ECMWF atmospheric model, one can still argue about the global validity of the model wind speed. Furthermore, it is desirable that the wind retrieval algorithm would perform satisfactorily against buoy wind measurements. To ensure that, the RA-2 collocations with available buoy wind measurements (as received through the Global Telecommunication System, GTS) were used to fine-tune the resulting algorithm during the same two months. The scale of the buoy observations is adjusted to RA-2 super-observation and model scales by averaging over five consecutive hourly measurements. The quality control procedure outlined by Bidlot et al. (2002) was used. The fine-tuning was done on a trial and error basis to find the optimal fit between the buoy winds and the RA-2 wind speeds as computed from (1) and (2). It was found that the most optimal fit, can be reached by adjusting U_m above as follows:

$$U_{10} = U_m + 1.4 U_m^{0.096} \exp(-0.32 U_m^{1.096}) \tag{3}$$

The proposed algorithm (1)-(3) is plotted as a continuous green curve in Fig. 6. Note that the final fit slightly deviated from the altimeter-model mean relation.
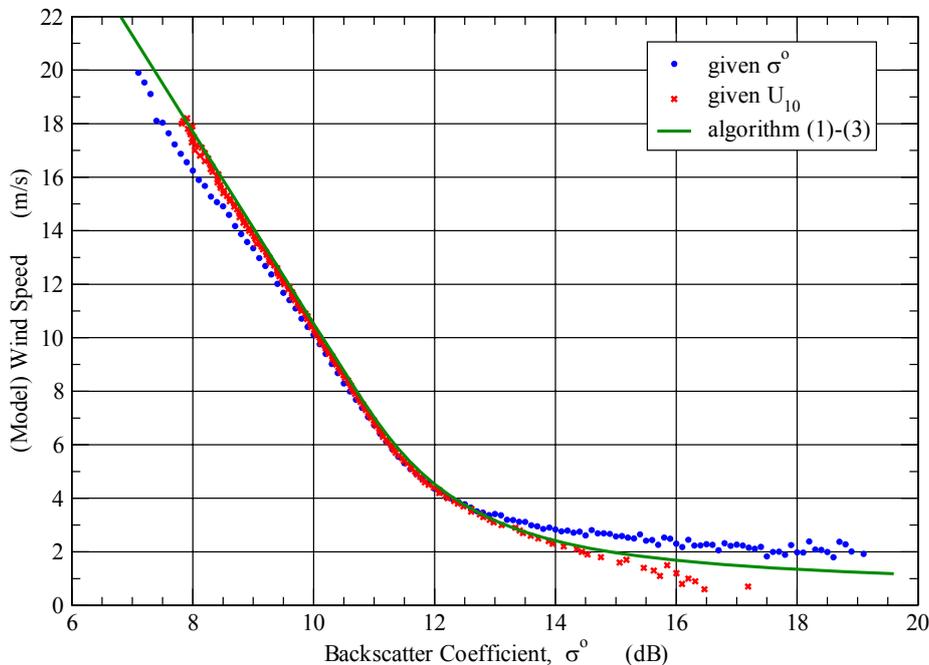
Figure 6: Relation between ECMWF model wind speed and ENVISAT RA-2 backscatter coefficient values during the period from 1 January - 28 February 2005. Blue dots are mean wind speed for given bins of backscatter coefficient; red crosses are mean backscatter coefficient for given bins of wind speed. Green line is the proposed algorithm in Equations (1)-(3).

4. Algorithm verification

Being an empirical model, the algorithm (1)-(3) needs extensive verification. The first set of verification is a reprocessing of two years (9 April 2003 - 9 April 2005) of ENVISAT RA-2 Ku-band σ^o observations. Equations (1)-(3) were used to derive U_{10}. The resulting winds are collocated with the ECMWF model counterparts. The time-series of the global wind speed bias defined as the difference between the altimeter and the model wind speeds from the original product computed using the MCW algorithm and the proposed algorithm of (1)-(3) are plotted in the upper panel of Fig. 7. The new algorithm produces wind speeds which are about 0.4 m·s^{-1} higher than MCW. The proposed algorithm suggests that, on average ECMWF model

underestimates surface wind speeds by about 0.25 m·s^{-1} during that period. Verification of the ECMWF wind speeds against buoy observations (e.g. Bidlot et al., 2002) gives a similar signal. The lower panel of Fig. 7 shows the same time-series but for the Northern Hemispheric (NH) Extra-Tropics (north of 20°N). It is clear that the same seasonal cycle does exist in both time-series. However, the difference between the two biases (plotted as the turquoise line) suggests that the new algorithm is able to eliminate part of the seasonal variation. Fig. 8 shows the time-series of the global scatter index, SI, (defined as the standard deviation of the difference between the two data sets normalised by the mean of the reference data set) between RA-2 and the model. It is clearly visible that the new algorithm performs better than the classical MCW algorithm with a SI reduction of about 6% during the whole period. Most of the improvement is in the Tropics between latitudes 20°N and 20°S (not shown) where light to medium wind speeds are the norm.
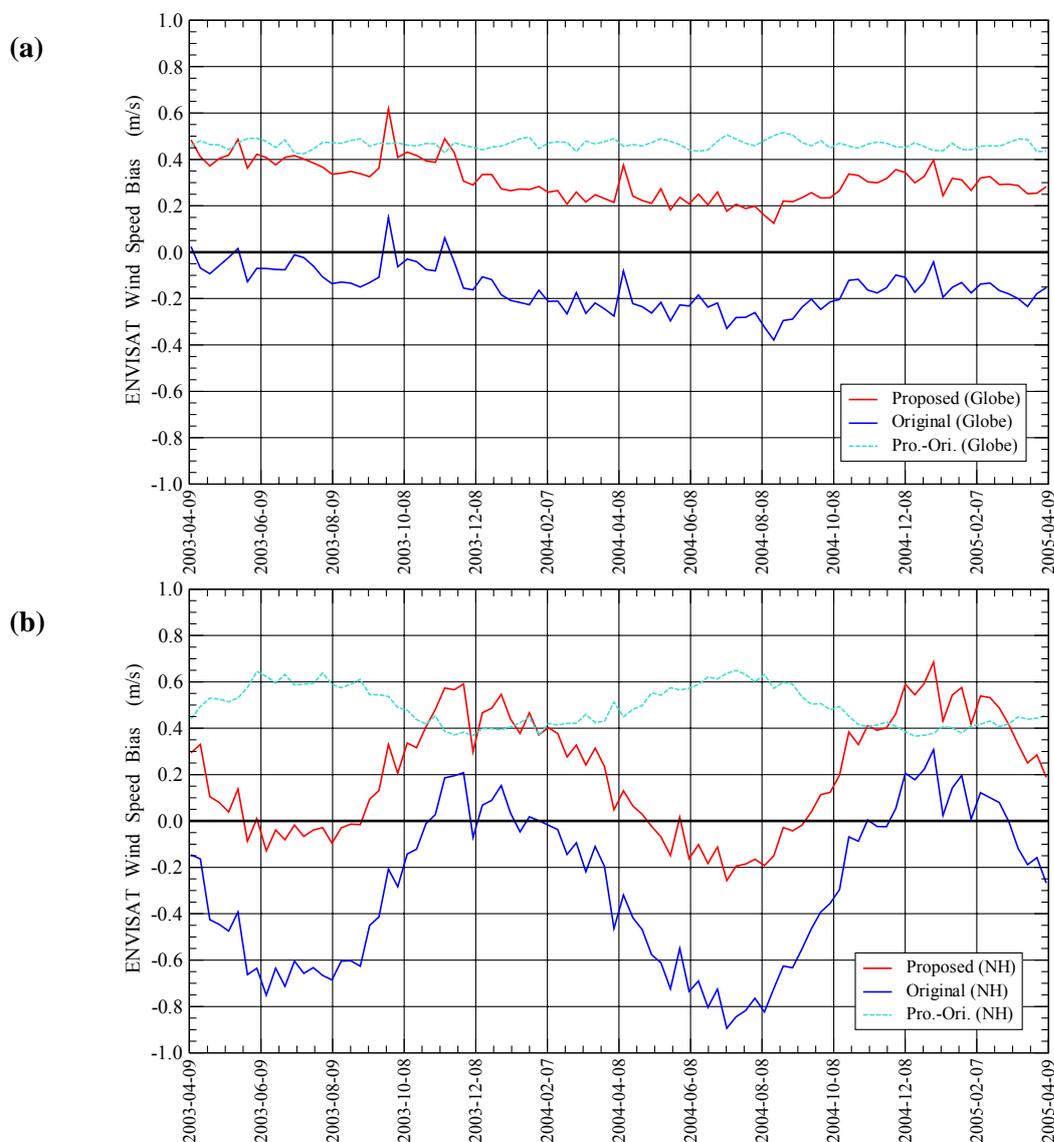
Figure 7: Time-series of the wind speed difference (bias) between ENVISAT RA-2 and ECMWF model from the original ESA product (blue) and as proposed in Equations (1)-(3) (red) over the period from 9 April 2003 and 9 April 2005 in the whole Globe (a) and in the Northern Hemispheric Extra-Tropics (b). The difference between the two lines is plotted as the turquoise dashed line.
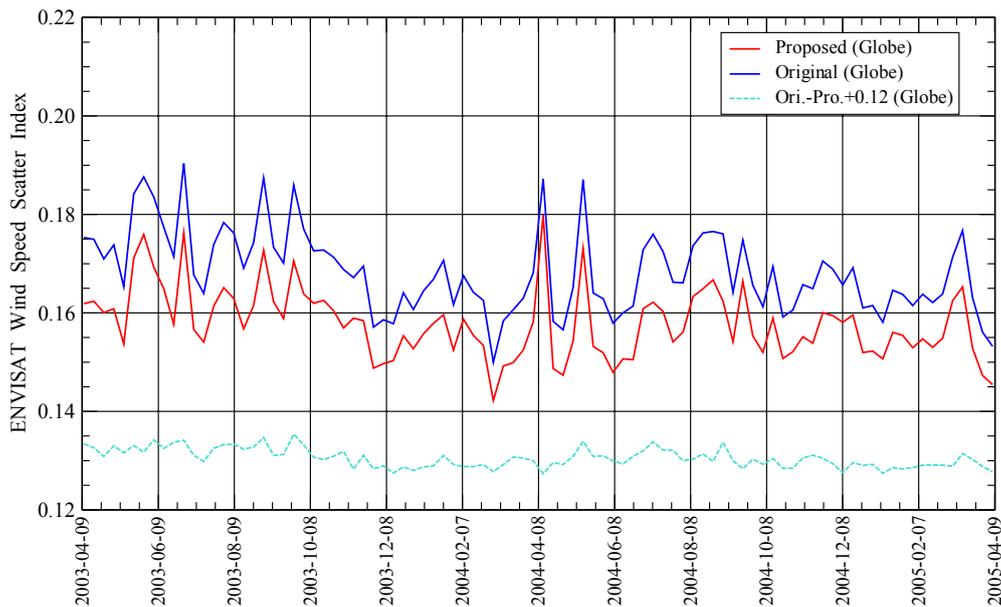
Figure 8: Time-series of the wind speed scatter index between ENVISAT RA-2 and ECMWF model from the original ESA product (blue) and as proposed in Equations (1)-(3) (red) over the period from 9 April 2003 and 9 April 2005 in the whole Globe. The difference between the scatter indexes of original and the proposed algorithms is plotted with a reference of the 0.12 value as the turquoise dashed line.

The same algorithm, without any modifications, was also applied to five years (16 July 1998 - 23 June 2003) of ERS-2 RA observations. Similar results (not shown) to those of ENVISAT were obtained. The exception was the period from late January to early March each year since 2000 due to the "sun-blinding effect" (see Abdalla and Hersbach, 2004) experienced by the ERS-2 platform after the loss of its gyroscopes, resulting in σ^o values of poor quality.

The real challenge, however, was the implementation of the proposed algorithm to Jason-1 RA. As mentioned earlier, the two-parameter algorithm of Gourrion et al. (2002) is used to retrieve wind speed from Jason-1 backscatter coefficients and significant wave heights. Global monitoring of Jason-1 RA Operational Sensor Data Record (OSDR) products carried out routinely at ECMWF suggests that Jason Ku-band σ^o is about 0.4 dB higher than that of ENVISAT. Therefore, Jason-1 σ^o values were reduced by this amount before applying the algorithm (1)-(3). More than 18 months (1 November 2003 - 9 March 2005) of Jason-1 data were used and compared to the ECMWF model. The time-series of the global SI for the original OSDR product and as retrieved using algorithm (1)-(3) are shown in Fig. 9. The proposed algorithm (with σ^o values reduced by 0.4 dB) produced less error over the whole period. This is an interesting result. There are two possible explanations for this. The significant wave height may not be enough by itself to represent the sea-state dependence (see discussion in Section 6). The possibility that the algorithm of Gourrion et al. (2002) needs further tuning cannot be ruled out as well.
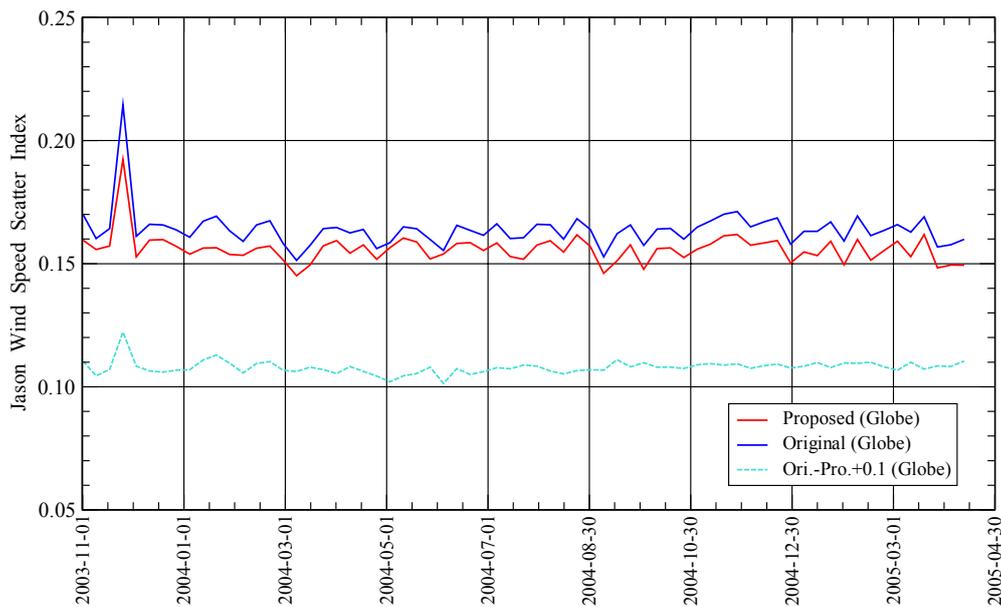
Figure 9: Time-series of the wind speed scatter index between Jason RA and ECMWF model from the original Jason product (blue) and as proposed in Equations (1)-(3) with backscatter-coefficient shifted by 0.4 dB (red) over the period from 1 November 2003 and 9 April 2005 in the whole Globe. The difference between the scatter indexes of original and the proposed algorithms is plotted with a reference of the 0.10 value as the turquoise dashed line.

The ENVISAT RA-2 wind speeds in the collocation data set (altimeter - buoy collocations) plotted in Fig. 2 were recomputed using the algorithm (1)-(3). The resulted scatter plot is shown in Fig. 10. The improvement in wind speed regime below about 10 m·s^{-1} is very clear in the plot. The few high wind speed observations are now aligned closer to the symmetric line. The bias is reduced by about 0.46 m·s^{-1} and the scatter index reduced by about 0.5%. Similar results and plot emerged from the ERS-2 comparison exercise (not shown). The algorithm (with σ^o values reduced by 0.4 dB) was also applied for the Jason-1 - buoy collocations presented in Fig. 3. The resulted scatter plot is shown in Fig. 11. While clear improvement can be seen at low wind speeds, the overall improvement from the original plot in Fig. 3 is less pronounced compared to the ENVISAT case. Summary of the improvements achieved by the proposed algorithm compared to the original algorithm with respect to buoy data is tabulated in Table 1.

Table 1: Impact of proposed algorithm on altimeter - buoy comparison

Altimeter	Period	Bias (m·s^{-1})		Scatter Index	
		Original	Proposed	Original	Proposed
ENVISAT	Jan. 2004 - Feb. 2005	-0.59	-0.13	0.1785	0.1696
ERS-2	Jan. 2000 - Feb. 2005	-0.44	+0.05	0.1991	0.1913
Jason-1	Oct. 2003 - Aug. 2005	-0.59	-0.40	0.1755	0.1741
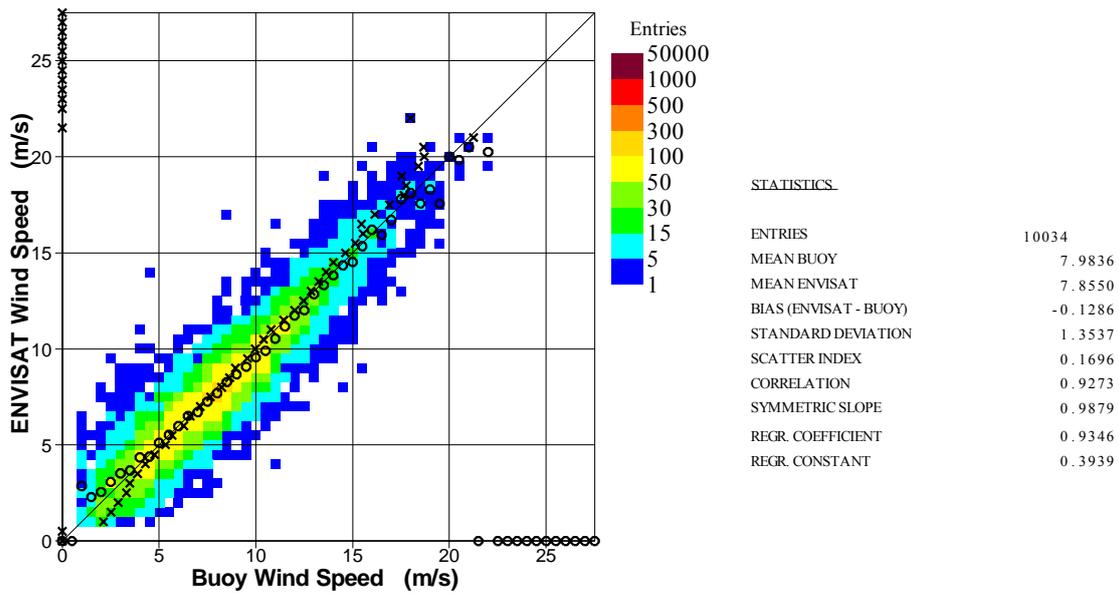
Figure 10: As in Figure 2 but ENVISAT RA-2 wind speed is computed from backscatter coefficients using Equations (1)-(3). For explanation of crosses and circles see Figure 1.
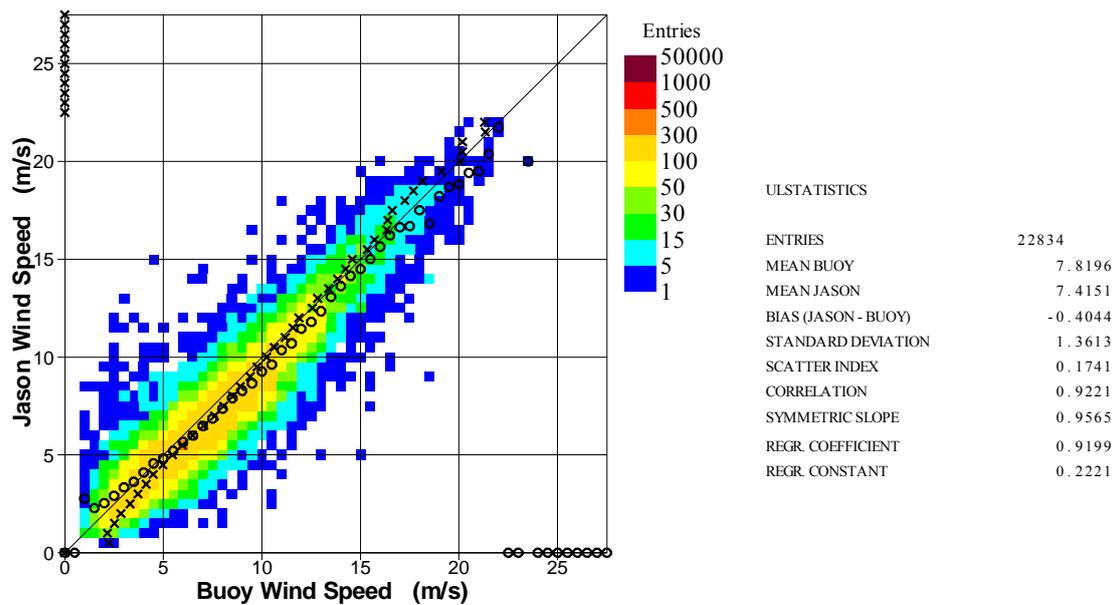
Figure 11: As in Figure 3 but Jason RA wind speed is computed from backscatter coefficients (shifted by 0.4 dB) using Equations (1)-(3). For explanation of crosses and circles see Figure 1.

5.   Implementation to ENVISAT RA-2

On 24 October 2005, the near real time RA-2 Level 1b and Level 2 Instrument Processing Facility (IPF) Version 5.02 processing chain was operationally implemented (c.f. EOO/EOX - Serco/Datamat, 2005). This processing chain introduced the algorithm (1)-(3) for the operational wind retrieval. Due to some practical limitations, the implementation was limited to σ^o values between 7.0 and 19.6 dB. Beyond those limits wind speed is assumed constant as can be seen in Fig. 12. This has adversely impacts the extremely low and high winds. Compared to algorithm (1)-(3), the MCW algorithm tends to underestimate low winds as well as high winds (see Fig. 12).
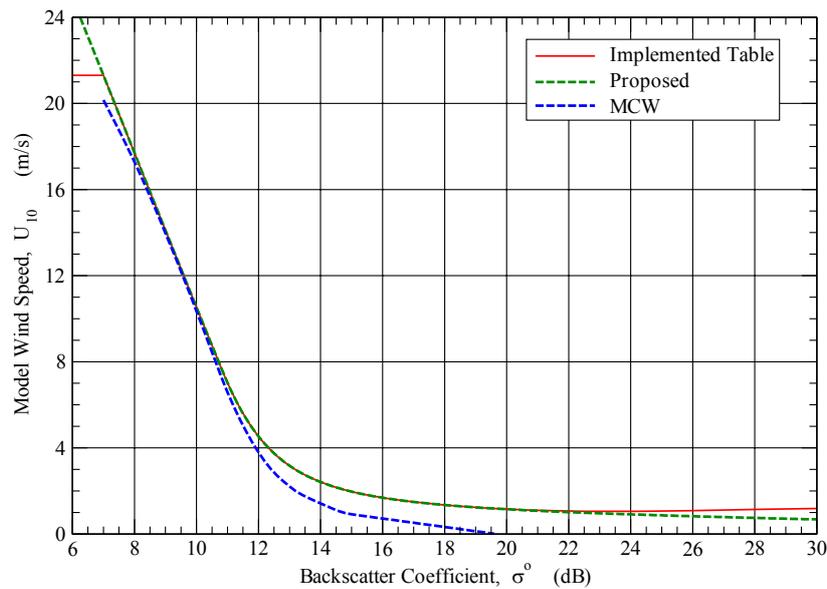
Figure 12: Relation between wind speed and backscatter coefficient (according to ENVISAT RA-2) values as implemented in ENVISAT RA-2 processing chain IPF Ver. 5.02 (red), as proposed in Equations (1)-(3) (green dashed). The classical MCW algorithm is also displayed (blue dashed) for comparison.

This implementation resulted in enhanced RA-2 wind speed characteristics. The comparisons against the model and the buoy observations show better agreement than before (similar to the scatter plots of Figs. 10 and 11). Fig. 13 shows that the RA-2 wind speed histogram after the implementation of IPF Ver. 5.02 (for 5 months only) is in better agreement with the model histogram of Fig. 4 (plotted on the same figure for comparison). The jump in the new histogram at wind speed slightly higher than 1 m·s^{-1}, can not be missed. This is due to the fact that the implementation of the algorithm applies an upper limit of to σ^o value as mentioned earlier (see Fig. 12). As a consequence, all of the lighter winds end up in that bin. A fine tuning to the algorithm to get rid of this jump can be carried out. However, there are some doubts whether very light wind speeds are able to cause wind wave generation (c.f. Kahma and Donelan, 1988). The better agreement between the new RA-2 histogram from one side and the histograms from the buoy and from model can not be missed in Fig. 14. Note that the histograms in Fig. 14 are from the altimeter - buoy collocation data set over about 4 months).

Fig. 15 shows the time-series of the global wind speed bias between the operational RA-2 and ECMWF model products for 12 months since the 1 November each year. While the bias from the period starting in 2003 and in 2004 show comparable negative bias (around -0.15 m·s^{-1}), the bias for the same period starting in 2005 (after the implementation of IPF Ver. 5.02) has a positive bias of about 0.23 m·s^{-1}. Similar time-series but for the standard deviation of the difference between RA-2 and the model are plotted in Fig. 16. It is clear that the standard deviation of the difference after the implementation of the IPF Ver. 5.02 is lower than the corresponding values in the last two years. The exception is about a month from the middle of December to the middle of January when the standard deviation of the difference from the recent period is comparable with that in the same period starting in 2003.
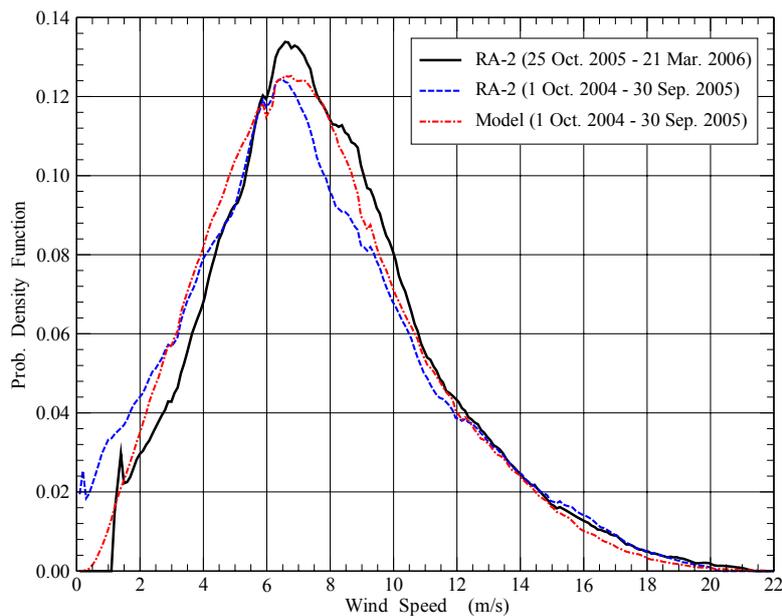
Figure 13: Probability density function of global wind speed from ENVISAT RA-2 after the implementation of the algorithm (1)-(3) (black thick) during the period from 25 October 2005 to 21 March 2006. Same curves of Figure 4 are reproduced (blue dashed and red dash-dotted) for comparison. The curve corresponding to the model collocations for the new period is not plotted as it is similar to the red dash-dotted curve here.
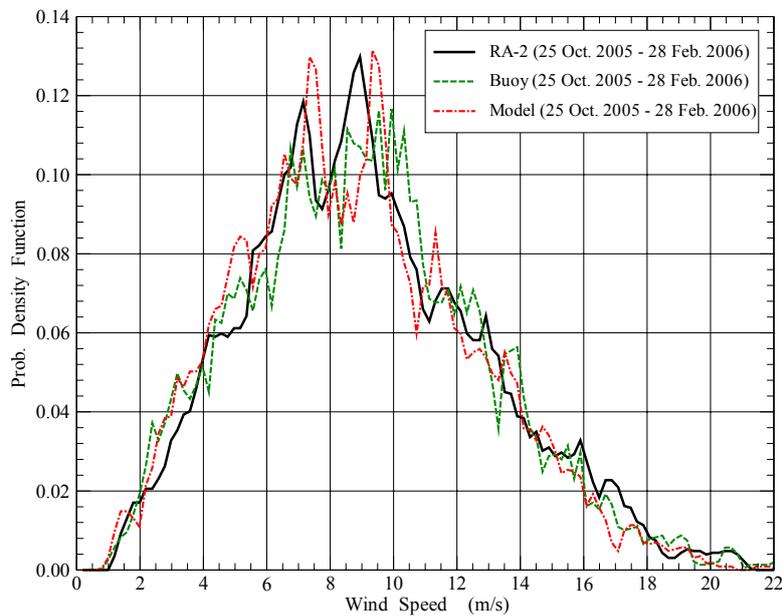
Figure 14: Probability density function of global wind speed from ENVISAT RA-2 after the implementation of the algorithm (1)-(3) (black thick) during the period from 25 October 2005 to 28 February 2006 for the altimeter-buoy collocations. The corresponding buoy (green dashed) and model (red dash-dotted) curves for the same data set are also plotted.
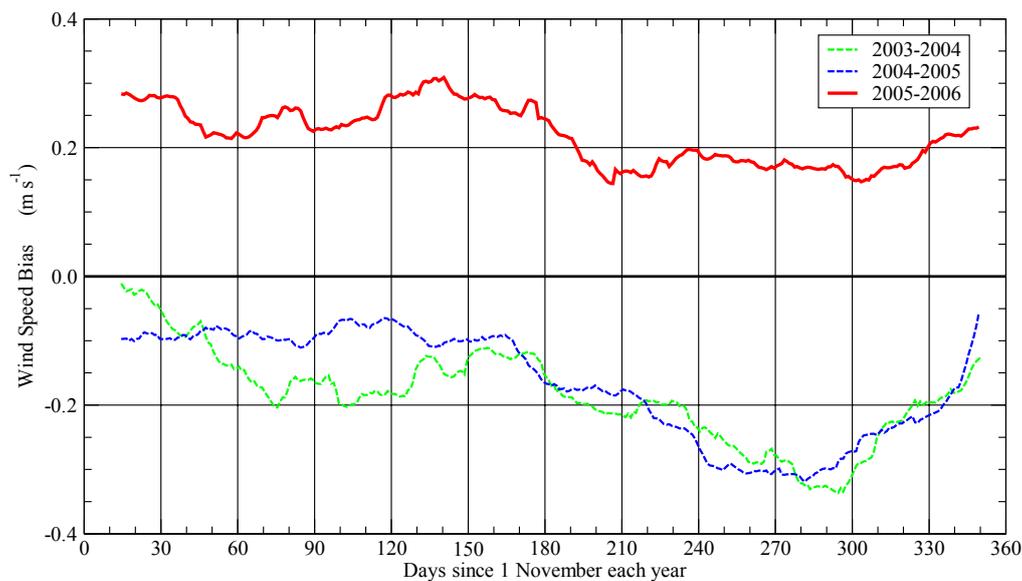
Figure 15: Time-series of the global wind speed difference (bias) between operational ENVISAT RA-2 and ECMWF model since 1 November of years 2003 (dashed green), 2004 (dashed blue) and 2005 (continuous red). Algorithm (1)-(3) was implemented (IPF Ver. 5.02) from 24 October 2005 onwards.
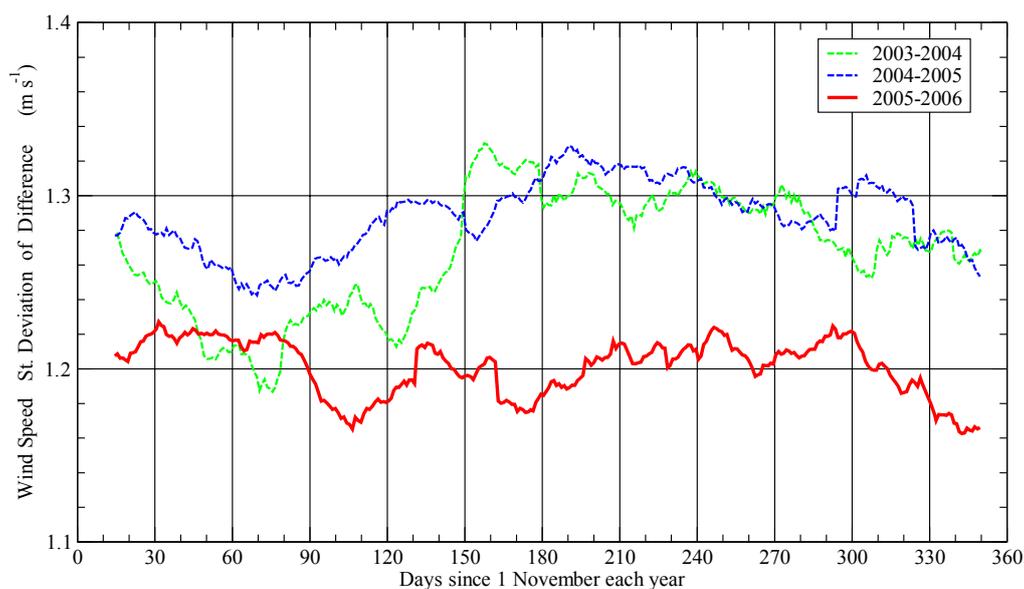
Figure 16: As in Fig. 15 but for the standard deviation of the difference.

6.   Significant wave height dependence

The sea-state dependence of the altimeter-derived surface wind was the subject of several research efforts (e.g. Glazman and Greysukh, 1993, Lefevre et al., 1994, Freilich and Challenor, 1994 and Hwang et al., 1998). The results of those studies show ranges of impacts from significant to no impact (e.g. Wu, 1999). Gourrion et al. (2002) argued quite convincingly that earlier studies reported no sea-state dependency (e.g. Wu, 1999) used a limited data set (GEOSAT - buoy collocations) and therefore were not able to detect such effect. Intuitively one would expect that sea state has an impact. The question however, would be: "is significant wave height, H_s, the proper parameter that can be related to this impact?" H_s is an integrated

parameter that includes both wind sea part (which is directly related to wind speed) and swell part (which may impact the altimeter wind retrieval). Therefore, unless there is a technique to separate those two different parts, it may not be possible to use the altimeter-derived H_s in wind retrieval algorithms. Even Gourrion et al. (2002), while introducing H_s in their two-parameter algorithm, warned that H_s may not be the best parameter to use.

ENVISAT RA-2 backscatter coefficients and significant wave heights (after quality control) were collocated with the ECMWF model surface wind speeds over a whole year (2005). Average wave heights were computed for each bin with $\Delta\sigma^o$ =0.1 dB and ΔU_{10} =0.1 m·s^{-1}. Bins of equal mean H_s values were plotted in Fig. 17 (plots of Fig. 6 are displayed as well for reference). Fig. 17 shows that for small wave heights (say less than 2 m), there is a correlation between wind speed and wave height for a given backscatter coefficient value. On the other hand, for wave heights above about 2 m, the dependence of the wind speed on H_s is very weak for any given σ^o value. Furthermore, Fig. 17 shows that there is a saturation σ^o value for each H_s which can not be exceeded irrespective of the wind speed. In other words, there is a threshold σ^o value for each H_s so that the wave height dependence does not hold anymore. Those threshold (or saturation) values were extracted from Fig. 17 and plotted against their corresponding H_s values in Fig. 18. It was not easy to extract the threshold σ^o value corresponding to H_s =1.5 m (if one exists). Although the relation in Fig. 18 may not be linear, a regression line was plotted.
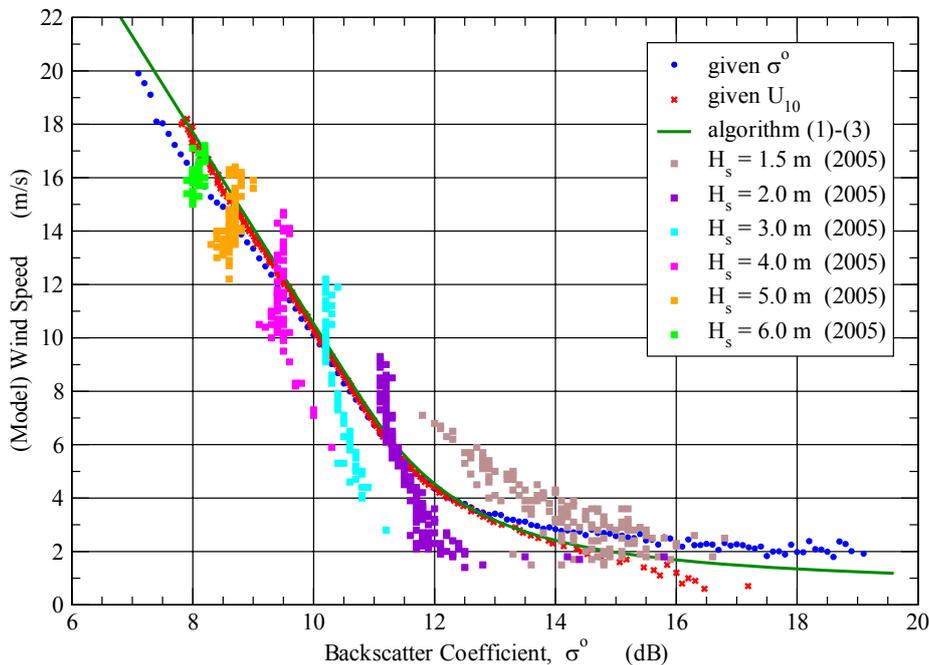
Figure 17: Same as Figure 6 superposed with the dependence of wind speed- backscatter-coefficient relationship on significant wave height. The relation is plotted for given equal significant wave height values binned in a way similar to the blue dots and red crosses (see Figure 6) but for the whole year of 2005.
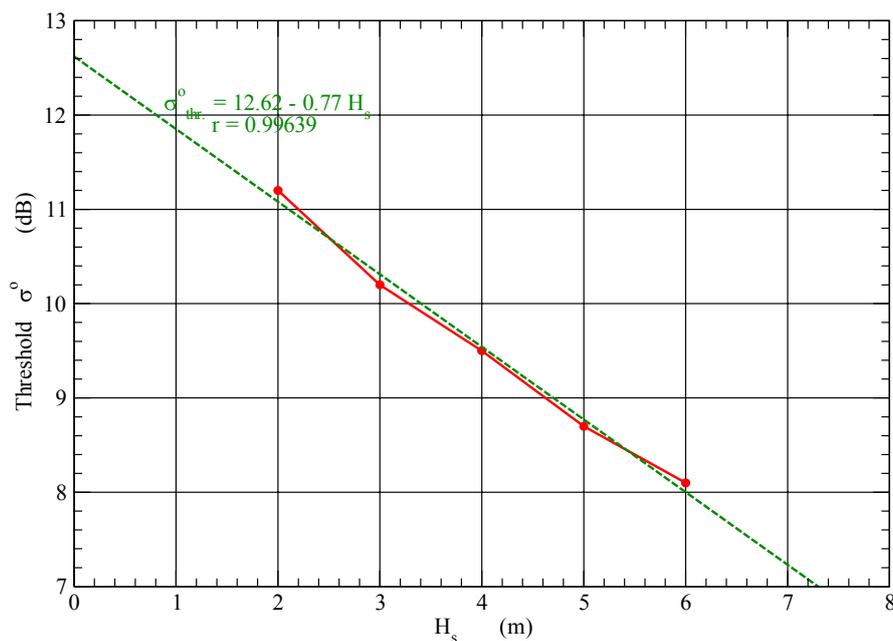
Figure 18: Threshold altimeter backscatter coefficient values at which the backscatter seems not to be affected by wind speed for given sea-state conditions (significant wave height values). Regression line is also plotted (green dashed).

7.   Conclusions

The modified Chelton-Wentz (MCW) algorithm for the retrieval of altimeter surface wind speed from Ku-band altimeters was fine tuned using two-month (January-February 2005) worth of ENVISAT altimeter (RA-2) - ECMWF model collocations. The new algorithm was later adjusted using RA-2 - buoy collocations during the same two months. The algorithm is given in Equations (1)-(3). The algorithm was extensively verified using several collocation data sets including the altimeter Ku-band backscatter coefficient from ENVISAT, ERS-2 and Jason-1 and the wind speed from ECMWF model and from buoy observations. The new algorithm increases altimeter wind speeds by about 0.40 m·s^{-1} compared to MCW algorithm. This is much in line with the expected correct global wind speeds. The proposed algorithm reduces the scatter index by about 5%. The algorithm performs even better than the two-parameter algorithm of Gourrion et al. (2002) implemented on Jason-1. The proposed algorithm was implemented for ENVISAT RA-2 on 24 October 2005. Verifications for about a year afterwards showed better performance in terms of wind speed retrieval.

One year worth of data showed that the use of significant wave height as a second parameter for the altimeter wind retrieval algorithms may not be a proper choice for high sea-state conditions. It seems that there is a saturation backscatter coefficient value for each significant wave height which can not be exceeded irrespective of the wind speed. This issue needs further investigation.

Acknowledgments

References

Abdalla, S. and Hersbach, H. (2004). *The technical support for global validation of ERS Wind and Wave Products at ECMWF*. ECMWF Final Report for ESA contract 15988/02/I-LG, 46 pp. Available online at: http://www.ecmwf.int/publications/

Bidlot, J.R., Holmes, D.J., Wittmann, P.A., Lalbeharry, R. and Chen, H.S. (2002). Intercomparison of the Performance of Operational Ocean Wave Forecasting Systems with Buoy Data. *Wea. and Forec.*, **17**, 287-310.

EOO/EOX - Serco/Datamat (2005). *Information to the Users regarding the Envisat RA2/MWR IPF version 5.02 and CMA 7.1*. Internet web page visited on 13 Dec. 2005, http://earth.esa.int/pcs/envisat/ra2/articles/RA2_MWR_IPF_5.02.html

Freilich, M. and Challenor, P. (1994). A New Approach for Determining Fully empirical altimeter wind speed model function. *J. Geophys. Res.*, **99**, 25051-25062.

Glazman, R. and Greysukh, A. (1993). Satellite Altimeter Measurements of Surface Wind. *J. Geophys. Res.*, **98**, 2475-2483.

Gourrion, J., Vandemark, D., Bailey, S., Chapron, B., Gommenginger, G.P., Challenor, P.G. and Srokosz, M.A. (2002). A Two-Parameter Wind Speed Algorithm for Ku-Band Altimeters. *J. Atmos. Oceanic Technol.*, **19**, 2030-2048.

Janssen, P.A.E.M., Abdalla, S. and Hersbach, H. (2003). Error Estimation of Buoy, Satellite and Model Wave Height Data. *ECMWF Technical Memorandum* No. 402. ECMWF, Reading, UK. Available online at: http://www.ecmwf.int/ publications/

Hwang, P., Teague, W., Jacobs, G. and Wang, D. (1998). A Statistical Comparison of Wind Speed, Wave Height and Wave Period Derived from Satellite Altimeters and Ocean Buoys in the Gulf of Mexico Region. *J. Geophys. Res.*, **103**, 10451-10468.

Kahma, K.K. and Donelan, M.A. (1988). A Laboratory Study of the Minimum Wind Speed for Wind Wave Generation, *J. Fluid Mech.*, **192**, 339-364.

Lefevre, J., Barckicke, J. and Menard, Y. (1994). A Significant Wave Height Dependent Function for TOPEX/Poseidon Wind Speed Retrieval, *J. Geophys. Res.*, **99**, 25035-25046.

Witter, D.L. and Chelton, D.B. (1991). A Geosat Altimeter Wind Speed Algorithm and a Method for Altimeter Wind Speed Algorithm Development. *J. Geophys. Res.*, **96**, 8853-8860.

Wu, J. (1999). On Wave Dependency of Altimeter Sea Returns – Weak Fetch Influence on Short Ocean Waves. *J. Atmos. Oceanic Technol.*, **16**, 373-378.

Young, I. (1999). Seasonal Variability of the Global Ocean Wind and Wave Climate. *Int. J. Climatol.*, **19**, 931-950.